East European Journal of Physics. 3. 465-473 (2024)
DOI:10.26565/2312-4334-2024-3-56 ISSN 2312-4334

RADIATION OF ELECTROMAGNETIC WAVES BY REGULAR AND BICONICAL DIPOLES WITH VARIABLE DISTRIBUTED SURFACE IMPEDANCE AND ARBITRARY EXCITATION

Mikhail V. Nesterenko*, Victor A. Katrich, Yurii V. Arkusha, Vladimir V. Katrich
V.N. Karazin Kharkiv National University, 4, Svobody Sq., Kharkiv, Ukraine, 61022
**Corresponding Author e-mail: mikhail.v.nesterenko@gmail.com*
Received June 5, 2024; revised July 16, 2024; accepted August 19, 2024

An approximate analytical solution of a problem concerning the radiation of electromagnetic waves by regular and biconical dipoles with constant and variable complex distributed surface impedance and arbitrary excitation is derived. Solution correctness is confirmed by satisfactory agreement of experimental and numerical results from well-known literary sources. Numerical results are given for the input characteristics and radiation fields of the dipoles in the cases of its symmetric and asymmetric excitation by a point source.
Keywords: *Regular dipole; Biconical dipole; Variable distributed surface impedance; Arbitrary excitation; Current distribution; Input characteristics; Radiation fields*
PACS: 02.70.Pt; 78.70Gq; 84.40.-x

Currently, a variety of single-frequency and multi-frequency antenna structures are used in mobile and stationary communication systems [1-3]. These can be antennas protruding beyond the body of an electronic device [4-10], patch antennas directly integrated into communication devices, for example, [11-21] and references therein. To create multi-band (multi-channel) antennas, researchers have repeatedly proposed the use of dipoles with an asymmetric excitation point [7, 9, 22-28]. But in many cases, designers take the path of combining several antenna structures operating at different frequencies into one system. This choice significantly complicates the design of the antenna element and is an undesirable factor on the path to its miniaturization. In order to reduce the weight and size parameters of the antenna structure, it was also proposed to change the radius of the cross section of the dipole along its length according to a certain law, for example, linear (biconical dipole) [29–42]. However, these publications are devoted to calculating the characteristics of ideally conducting dipoles excited at the geometric center by a concentrated electromotive force (EMF) (symmetrical dipoles). In [42], it is proposed, for example, to create a three-frequency structure to use three different-sized symmetrical biconical dipoles, made of pure gold.

In [43], using a generalized method of induced EMF, the authors obtained an approximate analytical solution to the problem of current distribution in an asymmetric biconical dipole with a distributed surface impedance and arbitrary excitation. A characteristic property of such antenna design is the possibility of resonant tuning to selected frequencies depending on the geometric and electrophysical parameters of the dipole. Analysis of the input characteristics of the proposed dipole antenna showed the possibility of practical application of this antenna for multi-band portable radio stations, base stations and other antenna systems, for example, in unmanned aerial vehicles.

In this paper, for the first time a most general approximate analytical solution to the problem of the radiation of electromagnetic waves by regular and biconical dipoles with a variable distributed surface impedance and arbitrary excitation is obtained. Thus, we will combine in one design all the advantages of asymmetric excitation, biconical geometry and the presence of a variable distributed surface impedance. The antenna characteristics will be modelled by using the numerical-analytical method, known as generalized method of induced EMF, proposed by the authors earlier in [25, 26].

PROBLEM FORMULATION AND SOLUTION OF THE INTEGRAL EQUATIONS

Let us limit ourselves by the linear law of the radius change along the dipole (Fig. 1), which, in its turn, is rather good approximation for another dependences $r(s)$, for example, exponential one, at small angles ψ. Let the dipole of the $2L$ length and the variable radius according to the function $r(s)$ is located in free space. It has the variable distributed internal linear impedance $z_i(s) = z_i^s(s) + z_i^a(s)$ and is excited by the electrical field $E_{0s}(s)$ of the given sources (tangential component). The monochromatic fields and currents depend on time t as $e^{i\omega t}$ ($\omega = 2\pi f$ is the circular frequency, f is the linear frequency, measured in Hz). We assume that the dipole stays electrically thin in the operating frequency band, i.e. $kr(s) << 1$, $r(s) << 2L$, where $k = 2\pi/\lambda$, λ is the wavelength in free space. Then the integral equation relatively to the $J(s)$ current for the impedance boundary condition on the dipole surface [38]:

$$\left(\frac{\mathrm{d}^2}{\mathrm{d}s^2} + k^2\right)\int_{-L}^{L} J(s')\frac{e^{-ik\tilde{R}(s,s')}}{\tilde{R}(s,s')}\mathrm{d}s' = -\frac{i\omega}{\cos\psi}\left[E_{0s}(s) - z_i(s)J(s)\right], \tag{1}$$

Cite as: M.V. Nesterenko, V.A. Katrich, Y.V. Arkusha, V.V. Katrich, East Eur. J. Phys. 3, 465 (2024), https://doi.org/10.26565/2312-4334-2024-3-56

where $\tilde{R}(s,s') = \sqrt{(s-s')^2 + r^2(s)}$, $\psi = (\psi_1 + \psi_2)/2$, s and s' are the local coordinates related to the dipole axis and surface. Note that at $r(s) = const = r$, equation (1) transforms into an equation for the current in an dipole of constant radius with a quasi-one-dimensional core $\tilde{R}(s,s') = \bar{R}(s,s') = \sqrt{(s-s')^2 + r^2}$.

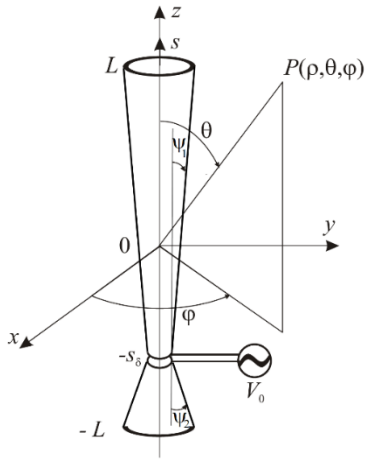

Figure 1. The geometry of the problem and accepted notations

To solve the equation (1) it is expedient to represent it in the form of the system of two coupled integral equations, concerning to the unknown currents $J^s(s)$ and $J^a(s)$, the first one of which is symmetrical, and the other – antisymmetrical relatively to the s variable:

$$\begin{cases} \left(\dfrac{\mathrm{d}^2}{\mathrm{d}s^2} + k^2\right) \displaystyle\int_{-L}^{L} J^s(s') \frac{e^{-ik\tilde{R}(s,s')}}{\tilde{R}(s,s')} \mathrm{d}s' = -\frac{i\omega}{\cos\psi} \left\{ [E_{0s}^s(s) - [z_i^s(s) J^s(s) + z_i^a(s) J^a(s)] \right\}, \\ \left(\dfrac{\mathrm{d}^2}{\mathrm{d}s^2} + k^2\right) \displaystyle\int_{-L}^{L} J^a(s') \frac{e^{-ik\tilde{R}(s,s')}}{\tilde{R}(s,s')} \mathrm{d}s' = -\frac{i\omega}{\cos\psi} \left\{ E_{0s}^a(s) - [z_i^s(s) J^a(s) + z_i^a(s) J^s(s)] \right\}. \end{cases} \tag{2}$$

The dipole currents can be presented as product of the unknown complex amplitudes $J_n^{s,a}$ and distribution functions $f_n^{s,a}(s')$ ($n = 0,1$) as

$$J^{s,a}(s') = J_0^{s,a} f_0^{s,a}(s') + J_1^{s,a} f_1^{s,a}(s'), \quad f_n^{s,a}(\pm L) = 0. \tag{3}$$

The solution of the equations system (2) can be obtained by the generalized method of induced EMF [25, 26]. To do so, let us multiply the left- and right- hand parts of the equations (2) by the functions $f_n^s(s)$ and $f_n^a(s)$, and integrate the resulting expressions over the dipole length. Thus, the following system of linear algebraic equations (SLAE) is obtained

$$\begin{cases} J_0^s Z_{00}^{s\Sigma} + J_1^s Z_{01}^{s\Sigma} + J_0^a \tilde{\tilde{Z}}_{00}^{sa} + J_1^a \tilde{\tilde{Z}}_{01}^{sa} = -(i\omega / 2k\cos\psi) E_0^s, \\ J_0^s Z_{10}^{s\Sigma} + J_1^s Z_{11}^{s\Sigma} + J_0^a \tilde{\tilde{Z}}_{10}^{sa} + J_1^a \tilde{\tilde{Z}}_{11}^{sa} = -(i\omega / 2k\cos\psi) E_1^s, \\ J_0^a Z_{00}^{a\Sigma} + J_1^a Z_{01}^{a\Sigma} + J_0^s \tilde{\tilde{Z}}_{00}^{as} + J_1^s \tilde{\tilde{Z}}_{01}^{as} = -(i\omega / 2k\cos\psi) E_0^a, \\ J_0^a Z_{10}^{a\Sigma} + J_1^a Z_{11}^{a\Sigma} + J_0^s \tilde{\tilde{Z}}_{10}^{as} + J_1^s \tilde{\tilde{Z}}_{11}^{as} = -(i\omega / 2k\cos\psi) E_1^a. \end{cases} \tag{4}$$

Here ($m = 0,1; n = 0,1$),

$$Z_{mn}^{s,a} = \frac{1}{2k\cos\psi} \left\{ -\frac{\mathrm{d}f_m^{s,a}(s)}{\mathrm{d}s} A_n^{s,a}(s) \Big|_{-L}^{L} + \int_{-L}^{L} \left[\frac{\mathrm{d}^2 f_m^{s,a}(s)}{\mathrm{d}s^2} + k^2 f_m^{s,a}(s) \right] A_n^{s,a}(s) \mathrm{d}s \right\}, \tag{5a}$$

$$A_n^{s,a}(s) = \int_{-L}^{L} f_n^{s,a}(s') \frac{e^{-ik\tilde{R}(s,s')}}{\tilde{R}(s,s')} \mathrm{d}s', \; E_m^{s,a} = \int_{-L}^{L} f_m^{s,a}(s) E_{0s}^{s,a}(s) \mathrm{d}s, \tag{5b}$$

$$\tilde{Z}_{mn}^{s,a} = -\frac{i\omega}{2k\cos\psi} \int_{-L}^{L} f_m^{s,a}(s) f_n^{s,a}(s) z_i^s(s) \mathrm{d}s, \quad Z_{mn}^{(s,a)\Sigma} = Z_{mn}^{s,a} + \tilde{Z}_{mn}^{s,a}, \; \tilde{\tilde{Z}}_{mn}^{\{sa\}} = -\frac{i\omega}{2k\cos\psi} \int_{-L}^{L} f_m^{\{s\}}(s) f_n^{\{a\}}(s) z_i^a(s) \mathrm{d}s, \tag{5c}$$

As can be seen, SLAE (4) is higher order than a similar SLAE for the case of a constant distributed surface impedance along the length of the dipole. That's why let us consider some particular solutions of the equations system (4), which we will need further.

1. The dipole with the impedance, constant along its length: $z_i^s(s) = const$, $z_i^a(s) = 0$. Then

$$J^{s,a}(s) = -\frac{i\omega}{2k\cos\psi}\left[\frac{E_0^{s,a}Z_{11}^{(s,a)\Sigma} - E_1^{s,a}Z_{01}^{(s,a)\Sigma}}{Z_{00}^{(s,a)\Sigma}Z_{11}^{(s,a)\Sigma} - Z_{10}^{(s,a)\Sigma}Z_{01}^{(s,a)\Sigma}} f_0^{s,a}(s) + \frac{E_1^{s,a}Z_{00}^{(s,a)\Sigma} - E_0^{s,a}Z_{10}^{(s,a)\Sigma}}{Z_{00}^{(s,a)\Sigma}Z_{11}^{(s,a)\Sigma} - Z_{10}^{(s,a)\Sigma}Z_{01}^{(s,a)\Sigma}} f_1^{s,a}(s)\right]. \tag{6}$$

2. The field of impressed sources has only the symmetrical component $E_{0s}^s(s)$ ($E_{0s}^a(s) = 0$). It is natural to suppose in this case, that it is sufficient to use only the first addendum – $J^a(s) = J_0^a f_0^a(s)$ in the antisymmetric component of the current in the dipole. Then the symmetrical and the antisymmetrical components of the current will be defined by the following formulas:

$$J^s(s) = -\frac{i\omega}{2k\cos\psi}\left[\frac{E_0^s Z_{11}^{sa\Sigma} - E_1^s Z_{01}^{sa\Sigma}}{Z_{00}^{sa\Sigma}Z_{11}^{sa\Sigma} - Z_{10}^{sa\Sigma}Z_{01}^{sa\Sigma}} f_0^s(s) + \frac{E_1^s Z_{00}^{sa\Sigma} - E_0^s Z_{10}^{sa\Sigma}}{Z_{00}^{sa\Sigma}Z_{11}^{sa\Sigma} - Z_{10}^{sa\Sigma}Z_{01}^{sa\Sigma}} f_1^s(s)\right], \tag{7a}$$

$$J^a(s) = -\frac{i\omega}{2k\cos\psi}\frac{E_0^s Z_{00}^{as\Sigma} + E_1^s Z_{01}^{as\Sigma}}{Z_{00}^{sa\Sigma}Z_{11}^{sa\Sigma} - Z_{10}^{sa\Sigma}Z_{01}^{sa\Sigma}} f_0^a(s), \tag{7b}$$

where

$$Z_{00}^{sa\Sigma} = Z_{00}^{s\Sigma} - \frac{(\tilde{\tilde{Z}}_{00}^{sa})^2}{Z_{00}^{a\Sigma}}, \quad Z_{01}^{sa\Sigma} = Z_{01}^{s\Sigma} - \frac{\tilde{\tilde{Z}}_{00}^{sa}\tilde{\tilde{Z}}_{01}^{as}}{Z_{00}^{a\Sigma}}, \quad Z_{10}^{sa\Sigma} = Z_{10}^{s\Sigma} - \frac{\tilde{\tilde{Z}}_{00}^{as}\tilde{\tilde{Z}}_{10}^{sa}}{Z_{00}^{a\Sigma}},$$
$$Z_{11}^{sa\Sigma} = Z_{11}^{s\Sigma} - \frac{\tilde{\tilde{Z}}_{10}^{sa}\tilde{\tilde{Z}}_{01}^{as}}{Z_{00}^{a\Sigma}}, \quad Z_{00}^{as\Sigma} = \frac{Z_{10}^{s\Sigma}\tilde{\tilde{Z}}_{01}^{as} - Z_{11}^{s\Sigma}\tilde{\tilde{Z}}_{00}^{as}}{Z_{00}^{a\Sigma}}, \quad Z_{01}^{as\Sigma} = \frac{Z_{01}^{s\Sigma}\tilde{\tilde{Z}}_{00}^{as} - Z_{00}^{s\Sigma}\tilde{\tilde{Z}}_{01}^{as}}{Z_{00}^{a\Sigma}}.$$

Let the dipole be excited in the point $s = -s_\delta$ by the voltage δ-generator with amplitude V_0, as shown in Fig. 1. Then

$$\begin{aligned} E_{0s}(s) &= V_0\delta(s + s_\delta) = E_{0s}^s(s) + E_{0s}^a(s), \\ E_{0s}^s(s) &= (V_0/2)\left[\delta(s + s_\delta) + \delta(s - s_\delta)\right], \\ E_{0s}^a(s) &= (V_0/2)\left[\delta(s + s_\delta) - \delta(s - s_\delta)\right], \end{aligned} \tag{8}$$

where δ is the Dirac delta function. Let us choose the functions $f_{0,1}^{s,a}(s)$ according to [26] in the following form:

$$\begin{aligned} f_0^s(s) &= \cos\tilde{k}s_\delta \sin\tilde{k}L\cos\tilde{k}s - (1/2)\cos\tilde{k}L(\sin\tilde{k}\,|\,s - s_\delta\,| + \sin\tilde{k}\,|\,s + s_\delta\,|), \\ f_0^a(s) &= \sin\tilde{k}s_\delta \cos\tilde{k}L\sin\tilde{k}s + (1/2)\sin\tilde{k}L(\sin\tilde{k}\,|\,s - s_\delta\,| - \sin\tilde{k}\,|\,s + s_\delta\,|), \end{aligned} \tag{9}$$

$$f_1^s(s) = \cos\tilde{k}s - \cos\tilde{k}L, \quad f_1^a(s) = \sin ks - (s/L)\sin kL, \tag{10}$$

where $\tilde{k} = k - \frac{i2\pi z_i^{av}}{Z_0\Omega}\left[\frac{1}{\cos\psi}\left(\frac{3}{2} - \frac{r_\delta}{2r_L}\right)\right]$, $\Omega = 2\ln\frac{2L}{r_L}$, $z_i^{av} = \frac{1}{2L}\int_{-L}^{L} z_i(s)\mathrm{d}s$ is the mean value of the internal impedance along the dipole length,, r_δ and r_L are the radii of the dipole in point $s = -s_\delta$ and in its end. The coefficients $Z_{mn}^{s,a}$ in the formulas (6), (7) can be obtained from (5) and the expressions $E_0^s = \cos\tilde{k}s_\delta \sin\tilde{k}\left(L - |\,s_\delta\,|\right)$, $E_1^s = \cos\tilde{k}s_\delta - \cos\tilde{k}L$, $E_0^a = -\sin\tilde{k}\,|s_\delta|\sin\tilde{k}\left(L - |\,s_\delta\,|\right)$, $E_1^a = \sin ks_\delta - (s_\delta/L)\sin kL$ for (6), $E_0^s = \sin\tilde{k}L$, $E_1^s = 1 - \cos\tilde{k}L$ for (7).

Note that the approximating functions in (4) adequately represent the real physical process if the electrical lengths of the dipole $(2L/\lambda) \le 1.4$. Two other approximating functions $f_2^s(s)$ and $f_2^a(s)$ valid in the range $1.4 < (2L/\lambda) \le 2.5$ can also be substituted in the expressions (3). These functions for the perfectly conducting dipole were obtained in [44] in the form

$$f_2^s(s) = \cos\frac{ks}{2} - \cos\frac{kL}{2}, \quad f_2^a(s) = \sin\frac{ks}{2} - \sin\frac{kL}{2}. \tag{11}$$

The input impedance $Z_{in} = R_{in} + iX_{in}$ and admittance $Y_{in}[\text{millimhos}] = G_{in} + iB_{in} = 10^3/Z_{in}$ can be presented as

$$Z_{in}[\text{Ohm}] = \frac{60i}{J_0^s f_0^s(s_\delta) + J_1^s f_1^s(s_\delta) + J_0^a f_0^a(s_\delta) + J_1^a f_1^a(s_\delta)}. \tag{12}$$

Then, the reflection coefficient in the antenna feeder with the wave impedance W is equal to

$$S_{11} = \frac{Z_{in} - \mathrm{W}}{Z_{in} + \mathrm{W}}, \tag{13}$$

and the voltage standing wave ratio is determined by the formula $\mathrm{VSWR} = \frac{1+|S_{11}|}{1-|S_{11}|}$.

The dipole radiation fields in all observation zones will be determined by the following expressions (in the spherical coordinate system ρ, θ, φ in Fig. 1):

$$\begin{aligned}
E_\rho(\rho,\theta) &= \frac{k}{\omega}\int_{-L}^{L} J(s)\frac{e^{-ikR(s)}}{R^3(s)}\left\{2R(s)\left[1+\frac{1}{ikR(s)}\right]\cos\theta - ik\rho\left[1+\frac{3}{ikR(s)}-\frac{3}{kR^2(s)}\right]s\sin^2\theta\right\}\mathrm{d}s,\\
E_\theta(\rho,\theta) &= -\frac{k\sin\theta}{\omega}\int_{-L}^{L} J(s)\frac{e^{-ikR(s)}}{R^3(s)}\left\{2R(s)\left[1+\frac{1}{ikR(s)}\right] - ik\rho\left[1+\frac{3}{ikR(s)}-\frac{3}{kR^2(s)}\right](\rho - s\cos\theta)\right\}\mathrm{d}s,\\
H_\varphi(\rho,\theta) &= \frac{ik^2\sin\theta}{\omega}\int_{-L}^{L} J(s)\frac{e^{-ikR(s)}}{R^2(s)}\left[1+\frac{1}{ikR(s)}\right]\rho\,\mathrm{d}s,\\
E_\varphi(\rho,\theta) &= H_\rho(\rho,\theta) = H_\theta(\rho,\theta) = 0,\\
R(s) &= \sqrt{\rho^2 - 2\rho s\cos\theta + s^2}.
\end{aligned} \tag{14}$$

In the far zone at $k\rho \to \infty$ and $\rho >> 2L$, expressions (11) are significantly simplified

$$E_\theta(\rho,\theta) = H_\varphi(\rho,\theta) = \frac{ik^2}{\omega}\sin\theta\frac{e^{-ik\rho}}{\rho}\int_{-L}^{L} J(s)e^{iks\cos\theta}\,\mathrm{d}s. \tag{15}$$

CONFIRMATION OF THE ADEQUACY OF THE PROPOSED MATHEMATICAL MODEL TO A REAL PHYSICAL PROCESS

1. Perfectly conducting regular dipole with symmetric excitation

The dependences of real G_{in} and imaginary B_{in} parts of the input admittance of the regular $r_\delta = r_L = r$ perfectly conducting dipole, excited in the point $s_\delta = 0$, from its electrical length $2L/\lambda$ have been calculated (Fig. 2).

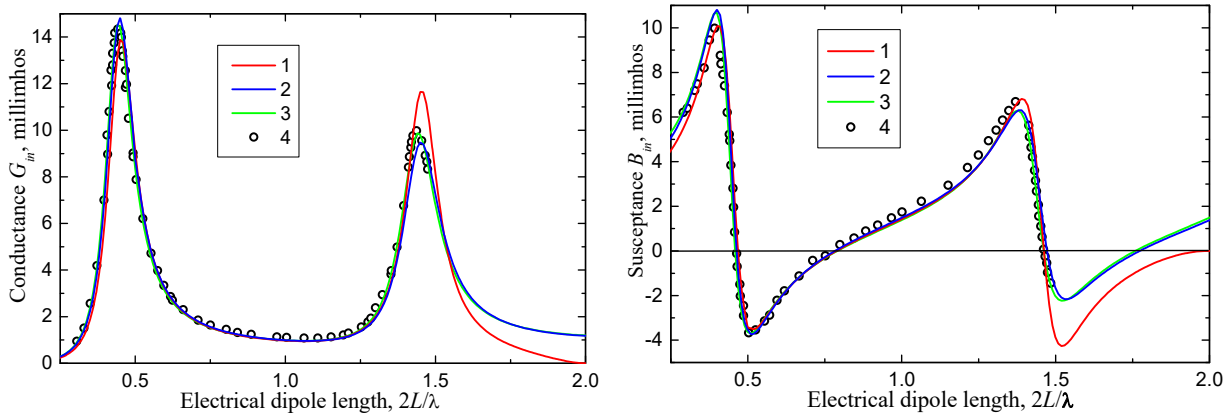

Figure 2. The input admittance versus electrical length of the symmetric regular perfectly conducting dipole at $f = 663$ MHz, $r/\lambda = 0.007022$, $s_\delta = 0$: 1–calculation (the functions (9) and (10)), 2–calculation (the functions (9), (10) and (11)), 3–calculation (the functions (16), 4–the experimental data [45]

Also, the calculated values, obtained by the moment method [22] at the current approximation by means of trigonometric functions of the whole region

$$J(s) = \sum_{n=1}^{N} J_n \sin\frac{n\pi(L+s)}{2L}, \tag{16}$$

are given here for comparison, what is more, to reach necessary accuracy the functions number in formula (16) are chosen to be equal $N = 24$.

2. Regular dipole with constant surface impedance and symmetric excitation

The dependences of real G_{in} and imaginary B_{in} parts of the input admittance of the regular $r_\delta = r_L = r$ dipole with constant distributed surface impedance, excited in the point $s_\delta = 0$, from its electrical length L/λ presented in Fig. 3 in comparison with experimental data.

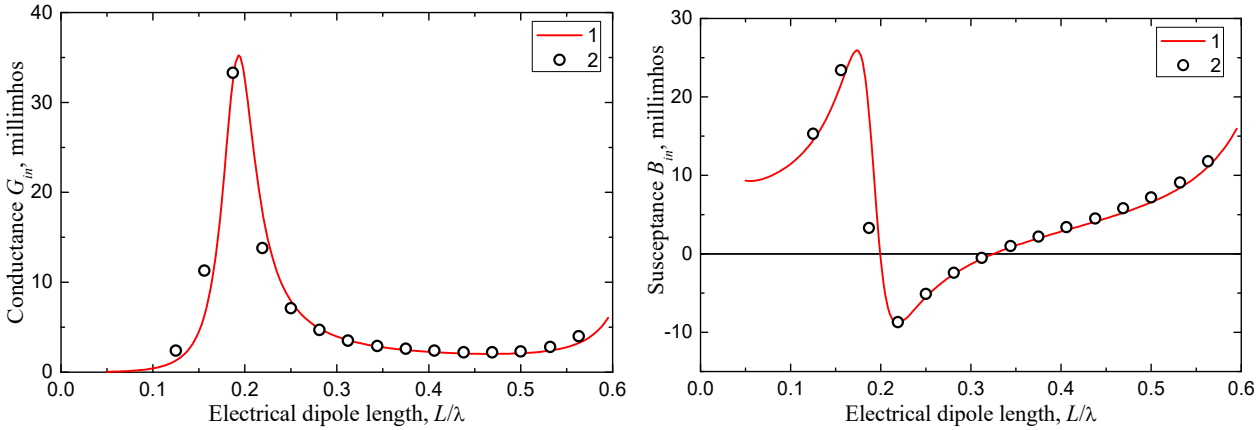

Figure 3. The input admittance versus electrical length of the symmetric regular metallic conductor of the radius $r_i = 0.3175$ cm, covered by the dielectrical ($\varepsilon = 9.0$) shell of the radius $r = 0.635$ cm at $f = 600$ MHz: 1–calculation (the functions (9) and (10)), 2–the experimental data [46].

NUMERICAL RESULTS

1. Regular dipole with variable surface impedance and symmetric excitation

Let the dipole be excited in the center ($s_\delta = 0$ in Fig. 1) by the hypothetical δ-generator of voltage V_0: $E^s_{0s}(s) = V_0\delta(s)$, $E^a_{0s}(s) = 0$. Then the current symmetrical component can be approximated by the function $f^s(s) = \sin\tilde{k}(L - |s|)$, where $\tilde{k} = k - \dfrac{i\bar{Z}^{av}_S[3/2 - r_\delta/(2r_L)]}{2r_L\cos\psi\ln(2L/r_L)}$, $\bar{Z}^{av}_S = \dfrac{1}{2L}\int\limits_{-L}^{L}\bar{Z}_S(s)\mathrm{d}s$ is the mean value of the dipole variable surface impedance, $\bar{Z}_S(s) = \bar{R}_S(s) + i\bar{X}_S(s) = 2\pi r_L z_i(s)/Z_0$ is the complex distributed surface impedance, normalized on the free space wave resistance $Z_0 = 120\pi$ Ohm. We use the following expression for the current antisymmetrical component [25]: $f^a(s) = \sin 2ks - 2\sin ks\cos kL$, and we represent the $\bar{Z}^{s,a}_S(s)$ functions in the form of $\bar{Z}^{s,a}_S(s) = \bar{Z}^{s,a}_S\phi^{s,a}(s)$.

Let us consider the following simple functions of the impedance distribution (which are realized rather easily in practice) as an example: $\phi^s(s) = 1$ – the distribution, constant along the dipole, $\phi^a(s) = \mathrm{sign}s = (|s|/s)$ – the step-function alternating distribution. Substituting $f^{s,a}(s)$ and $\phi^{s,a}(s)$ into the expressions (5) and (7), we obtain the formula for the current in the dipole with these laws of impedance distribution (the lower indices "mn" in (5) are omitted):

$$J(s) = -\frac{i\omega}{2k}V_0\sin\tilde{k}L\left[\frac{(Z^a + \tilde{Z}^a)\sin\tilde{k}(L - |s|) - \tilde{\tilde{Z}}^{sa}(\sin 2ks - 2\sin ks\cos kL)}{(Z^s + \tilde{Z}^s)(Z^a + \tilde{Z}^a) - (\tilde{\tilde{Z}}^{sa})^2}\right], \tag{17}$$

where $r(s) = const = r$,

$$Z^s = \frac{\tilde{k}}{k}[A^s(L) - \cos\tilde{k}LA^s(0)] + \frac{k^2 - \tilde{k}^2}{2k}\int\limits_{-L}^{L}f^s(s)A^s(s)\mathrm{d}s,\ Z^a = 2\sin^2 kLA^a(L) - \frac{3}{2}k\int\limits_{-L}^{L}\sin 2ks\,A^a(s)\mathrm{d}s,$$

$$A^{s,a}(s) = \int\limits_{-L}^{L}f^{s,a}(s')\frac{e^{-ik\bar{R}(s,s')}}{\bar{R}(s,s')}\mathrm{d}s',$$

$$\tilde{Z}^s = \frac{\bar{Z}^s_S}{i2\tilde{k}r}(2\tilde{k}L - \sin 2\tilde{k}L),\ \tilde{Z}^a = \frac{\bar{Z}^s_S}{ikr}\left(3kL - \frac{\sin 4kL}{12} - \frac{7}{3}\sin 2kL + 2kL\cos 2kL\right),$$

$$\tilde{\tilde{Z}}^{sa} = \frac{2\bar{Z}^a_S}{i\tilde{k}r}\left(\frac{2k^2\sin\tilde{k}L - k\tilde{k}\sin 2kL}{4k^2 - \tilde{k}^2} - 2\cos kL\frac{k^2\sin\tilde{k}L - k\tilde{k}\sin kL}{k^2 - \tilde{k}^2}\right).$$

Fig. 4 represents the dependences of the reflection coefficient $|S_{11}|$ from $\bar{X}_S^a$ at $\bar{X}_S^s = const$ in the feeder line with W =50 Ohm. As it is seen from graphics, there is a combinations of the values $\bar{X}_S^s$ and $\bar{X}_S^a$ for value $2L = 0.25\lambda$ (quarter-wave dipole), at which the reflection coefficient is minimum, that is, the dipole is tuned into resonance. The dependences $|S_{11}|(f)$ in the band of frequencies (Fig. 5) have been calculated in order to ground reliability of the obtained approximate analytical expression (13). Figs. 5, 6 also represent the calculated data, obtained by the method of finite elements, realized in the program "ANSYS HFSS".

The dipoles represent themselves metallic conductors of the radius r_i, covered by the layer of the magnetodielectric of the thickness $r - r_i$. The materials of the covering for one and the other arms of the dipoles on the frequency $f = 3\,\text{GHz}$ have the following electrophysical parameters [47]: 1) dielectric **Al₂O₃**, $\varepsilon_1 = 10 - i0.015$, $\mu_1 = 1.0$; 2) ferrite **2CX 1**, $\varepsilon_2 = 10.6 - i0.068$, $\mu_2 = 24.0$. The calculations of the values of the surface impedance components give the following results at these parameters of the magnetodielectrics due to the corresponding formula from [25]:

$$\bar{Z}_S = -i\sqrt{\frac{\mu}{\varepsilon}}\,\frac{I_0(k_1 r)N_0(k_1 r_i) - I_0(k_1 r_i)N_0(k_1 r)}{I_1(k_1 r)N_0(k_1 r_i) - I_0(k_1 r_i)N_1(k_1 r)}. \tag{18}$$

Here $k_1 = 2\pi\sqrt{\varepsilon\mu}/\lambda$, $\varepsilon = \varepsilon' - i\varepsilon''$ and $\mu = \mu' - i\mu''$ are the electro-physical parameters of the coating material, r_i is the inner conductor radius, r is the outer radius of coverage, I_n, N_n are the Bessel and Neumann functions of corresponding orders. Then for $2L = 0.25\lambda$ and $(r_i / r) = 0.5$ $\bar{Z}_S^s = 10^{-6} + i0.09$, $\bar{Z}_S^a = 10^{-6} + i0.08$. As it follows from the plots in Figs. 4, 5, these values are close to the corresponding ratios between $\bar{X}_S^s$ and $\bar{X}_S^a$ for tuning the dipoles into resonance at the frequency $f = 3\,\text{GHz}$.

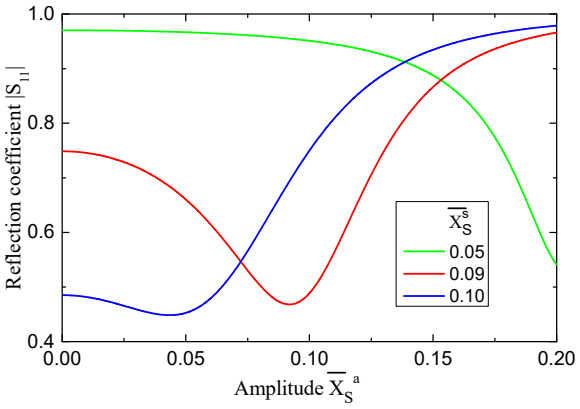

Figure 4. The reflection coefficient versus amplitude of the antisymmetrical surface impedance at $f = 3\,\text{GHz}$, $2L = 0.25\lambda$, $(L / r) = 75$

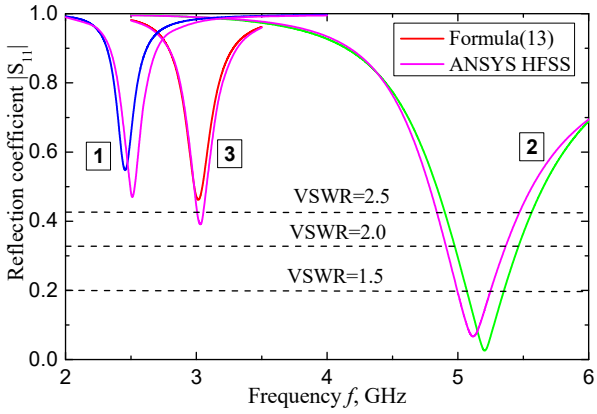

Figure 5. The reflection coefficient versus frequency at W =50 Ohm $2L = 0.25\lambda$, $(L / r) = 75$: 1 - 2CX 1 (both arms), 2 - Al_2O_3 (both arms), 3 - 2CX 1 + Al_2O_3 (first arm + second arm)

Finally, Fig. 6 shows the current distribution along a dipole with an asymmetric surface impedance in comparison with calculations using the "ANSYS HFSS" program, and Fig. 7 shows the spatial distribution of the radiation field in far zone of such a dipole in comparison with a perfectly conducting half-wave dipole.

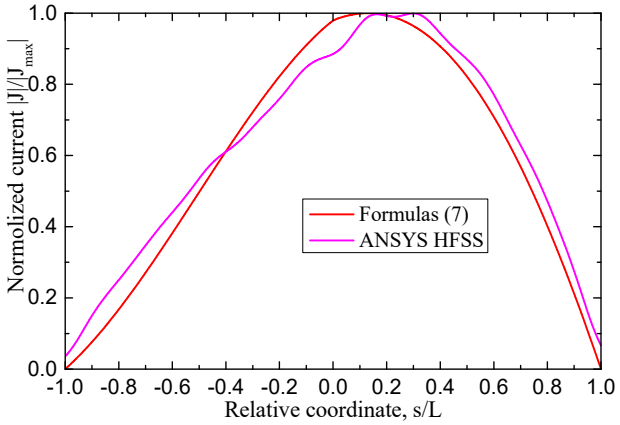

Figure 6. The current distribution along the dipole for the case 2CX 1 + Al_2O_3 (first arm + second arm) at $f = 3\,\text{GHz}$, $2L = 0.25\lambda$, $(L / r) = 75$

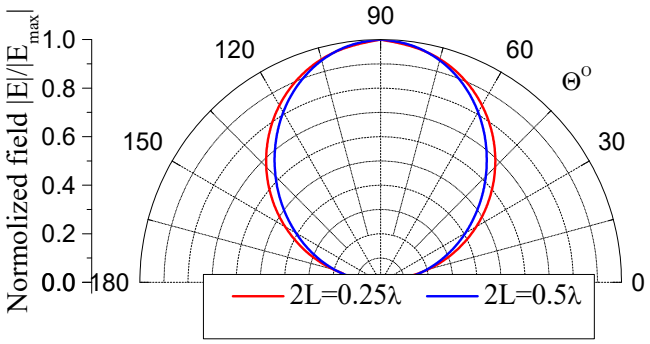

Figure 7. The spatial distribution of the dipole radiation field at $f = 3$GHz , $(L/r) = 75$ for the cases: 1) $2L = 0.25\lambda$, 2CX 1 + Al_2O_3 (first arm + second arm); 2) $2L = 0.5\lambda$ $\bar{Z}_S^{s,a} = 0$

2. Perfectly conducting biconical dipole with asymmetric excitation

Let us present the input characteristics (modulus of the reflection coefficient $|S_{11}|$ in the supply feeder line with wave resistance W =50 Ohm) of an asymmetric biconical perfectly conducting dipole with dimensions $2L$ =138 mm, r_δ =1 mm, r_L =3 mm (Fig. 8). This choice of the dipole length is due to the condition of the first resonance at the frequency f =0.9 GHz. Note that for a regular dipole with a radius r =2 mm, its length would be equal to $2L$ =156 mm. As can be seen from the graphs, an asymmetric biconical dipole (with smaller geometric length than a regular dipole) is also resonant at two or more frequencies. Moreover, this tendency will increase with increasing the angle ψ . Also, if the dipole has a distributed surface impedance of the inductive type, then its resonant length will be even less [26].

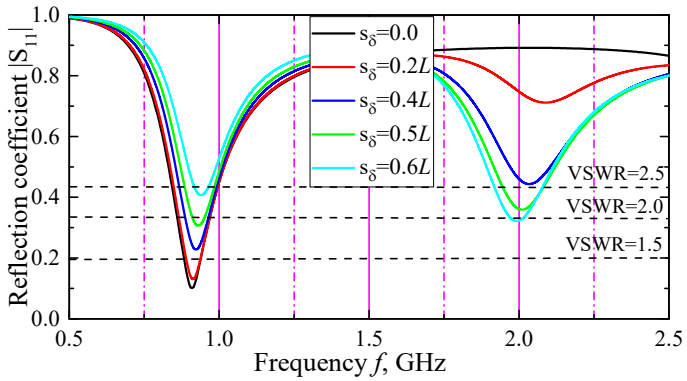

Figure 8. The reflection coefficient in the supply feeder line versus frequency for different positions of the excitation point s_δ at $2L$ =138 mm, r_δ =1 mm, r_L =3 mm, $\bar{Z}_S^{s,a} = 0$

Fig. 9 shows the spatial distribution of the radiation field of a dipole with an asymmetric excitation in comparison with calculations using the "ANSYS HFSS" program. As can be seen, the spatial distribution of the radiated field in this case has a two-lobe shape, and the level of the lobes can be changed by introducing a complex distributed surface impedance.

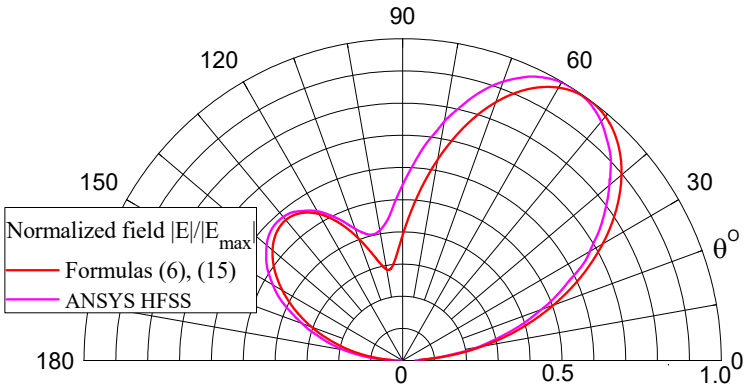

Figure 9. The spatial distribution of the dipole radiation field at $f = 0.9$GHz , $s_\delta = 0.2L$, $2L$ =138 mm, r_δ =1 mm, r_L =3 mm, $\bar{Z}_S^{s,a} = 0$

CONCLUSIONS

An approximate analytical solution of a problem concerning a current distribution, input characteristics and radiation fields of the regular and biconical dipoles with constant and variable complex distributed surface impedance and arbitrary excitation derived in the thin-wire approximation. The solution was carried out by the generalized method of induced EMF. Solution correctness is confirmed by satisfactory agreement of experimental results from well-known literary sources, and also of numerical results, performed using the moment method and using a commercial program "ANSYS HFSS". However, the use of commercial programs for dipoles, the electro-physical parameters of which depend on frequency f, raises serious doubts. This could be, for example, material TDK IR-E110 [48], which at the frequency band $f = 7 \div 12$ GHz are $\varepsilon_1 = 8.84 - i0.084$ and $\mu_1 = 2.42 - 0.0825 f[\mathrm{GHz}] - i0.994$. The solution presented in the paper is free of such shortcomings, moreover, the calculation time is tens of times (depending on the structure under consideration) less than that of direct numerical methods and commercial programs. The characteristic property of the antenna is the possibility of resonant tuning to the selected frequencies (depending on the geometric and electro-physical parameters of the dipole), which does not decrease the noise-resistant properties as compared with broadband antennas. Numerical results are given for the input characteristics and radiation fields of the dipoles with constant and variable distributed surface impedance in the cases of its symmetric and asymmetric excitation by a point source. Analysis of electrodynamic characteristics of the proposed dipole antennas has proved the possibility of practical applications of these antennas for multi-band portable radio stations, base stations and other antenna structures, for example, for antenna systems of unmanned aerial vehicles due to their small size and low weight compared to perfectly conducting regular dipoles.

ORCID

Mikhail V. Nesterenko, https://orcid.org/0000-0002-1297-9119; **Victor A. Katrich**, https://orcid.org/0000-0001-5429-6124

REFERENCES

[1] Z. N. Chen, *Antennas for portable devices*, Chichester, (England: Wiley, 2007).
[2] K. Fujimoto, and J. R. James, *Mobile antenna systems handbook*, (London, England: Artech House, 2008).
[3] Z. Zhang, *Antenna design for mobile devices*, (London, England: Wiley, 2017).
[4] G. Zhou, and B. Yildirim, "A multi-band fixed cellular phone antenna," in: Proc. IEEE AP-S Int. Symp. **1**, 112 (1999). https://doi.org/10.1109/APS.1999.789095
[5] N. Odachi, S. Sekine, H. Shoki, and Y. Suzuki, "A rod antenna with a meander element for hand-held phone," in: Proc. IEEE AP-S Int. Symp. **3**, 1682 (2000). https://doi.org/10.1109/APS.2000.874565
[6] H.-C. Tung, C.-Y. Fang, and K.-L. Wong, "Dual-band inverted-L monopole antenna for GSM/DCS mobile phone," in: Proc. IEEE AP-S Int. Symp. **3**, 30-33 (2002). https://doi.org/10.1109/APS.2002.1018149
[7] C. Song, Y. Huang, J. Zhou, P. Carter, S. Yuan, Q. Xu, and Z. Fei, "Matching network elimination in broadband rectennas for high-efficiency wireless power transfer and energy harvesting," IEEE Trans. Industrial Electronics, **64**, 3950-3961 (2017). https://doi.org/10.1109/TIE.2016.2645505
[8] K. Paramayudha, S. J. Chen, T. Kaufmann, W. Withayachumnankul, and C. Fumeaux, "Triple-band reconfigurable low-profile monopolar antenna with independent tenability," IEEE Open J. Antennas Propag. **1**, 47-56 (2020). https://doi.org/10.1109/OJAP.2020.2977662
[9] W. Hu, T. Feng, S. Gao, L. Wen, Q. Luo, P. Fei, Y. Liu, and X. Yang, "Wideband circularly polarized antenna using single-arm coupled asymmetric dipoles," IEEE Trans. Antennas Propag. **68**, 5104-5113 (2020). https://doi.org/10.1109/TAP.2020.2975275
[10] Y. Luo, and Y. Liu, "Nona-band antenna with small nonground portion for full-view display mobile phones," IEEE Trans. Antennas Propag. **68**, 7624-7629 (2020). https://doi.org/10.1109/TAP.2020.2989874
[11] S. Wang, and Z. Du, "A dual-antenna system for LTE/WWAN/WLAN/WiMAX smartphone applications," IEEE Antennas Wireless Propag. Lett. **14**, 1443-1446 (2015). https://doi.org/10.1109/LAWP.2015.2411253
[12] R. Tang, and Z. Du, "Wideband monopole without lumped elements for octa-band narrow-frame LTE smartphone," IEEE Antennas Wireless Propag. Lett. **16**, 720-723 (2017). https://doi.org/10.1109/LAWP.2016.2600761
[13] Y. Yang, Z. Zhao, W. Yang, Z. Nie, and Q.-H. Liu, "Compact multimode monopole antenna for metal-rimmed mobile phones," IEEE Trans. Antennas Propag. **65**, 2297-2304 (2017). https://doi.org/10.1109/TAP.2017.2679059
[14] Y. Liu, P. Liu, Z. Meng, L. Wang, and Y. Li, "A planar printed nona-band loop-monopole reconfigurable antenna for mobile handsets," IEEE Antennas Wireless Propag. Lett. **17**, 1575-1579 (2018). https://doi.org/10.1109/LAWP.2018.2856459
[15] D. Huang, Z. Du, and Y. Wang, "A quad-antenna system for 4G/5G/GPS metal frame mobile phones," IEEE Antennas Wireless Propag. Lett. **18**, 1586-1590 (2019). https://doi.org/10.1109/LAWP.2019.2924322
[16] Q. Tan, and F-C. Chen, "Triband circularly polarized antenna using a single patch," IEEE Antennas Wireless Propag. Lett. **19**, 2013-2017 (2020). https://doi.org/10.1109/LAWP.2020.3014961
[17] R.M. Moreno, J. Kurvinen, J. Ala-Laurinaho, A. Khripkov, J. Ilvonen, J. van Wonterghem, and V. Viikari, "Dual-polarized mm-wave endfire chain-slot antenna for mobile devices," IEEE Trans. Antennas Propag. **69**, 25-34 (2021). https://doi.org/10.1109/TAP.2020.3001434
[18] L. Chang, G. Zhang, and H. Wang, "Triple-band microstrip patch antenna and its four-antenna module based on half-mode patch for 5Gx4 MIMO operation," IEEE Trans. Antennas Propag. **70**, 67-74 (2022). https://doi.org/10.1109/TAP.2021.3090572
[19] C. Sahana, D. Nirmala, and M. Jayakumar, "Dual-band circularly polarized annular ring patch antenna for GPS-aided GEO-augmented navigation receivers," IEEE Antennas Wireless Propag. Lett. **21**, 1737-1741 (2022). https://doi.org/10.1109/LAWP.2022.3178980
[20] R. Lakshmanan, S. Mridula, A. Pradeep, and K. Neema, "Ultra compact flexible monopole antennas for tri-band applications," Prog. Electromagn. Res. C, **130**, 43-55 (2023). http://dx.doi.org/10.2528/PIERC22110906

[21] A. Khade, M. Trimukhe, S. Verblkar, and R. K. Gupta, "Miniaturization of printed rectangular monopole antenna by using slots for triple band applications," Prog. Electromagn. Res. C, **130**, 155-167 (2023). http://dx.doi.org/10.2528/PIERC22122401
[22] R. W. P. King, and T. T. Wu, "The cylindrical antenna with arbitrary driving point," IEEE Trans. Antennas Propag. **13**, 710-718 (1965). https://doi.org/10.1109/TAP.1965.1138531
[23] B. D. Popovic, "On polynomial approximation of current along thin asymmetrical cylindrical dipoles," IEEE Trans. Antennas Propag. **19**, 117-120 (1971). https://doi.org/10.1109/TAP.1971.1139879
[24] Y. Wang, S. Xu, and D. H. Werner, "1 bit dual-polarized reconfigurable transmitarray antenna using asymmetric dipole elements with parasitic bypass dipoles," IEEE Trans. Antennas Propag. **69**, 1188-1192 (2021). https://doi.org/10.1109/TAP.2020.3005713
[25] M. V. Nesterenko, V. A. Katrich, Y M. Penkin, V. M. Dakhov, and S. L. Berdnik, *Thin Impedance Vibrators. Theory and Applications*, (Springer Science+Business Media, New York, 2011).
[26] M. V. Nesterenko, V. A. Katrich, S. L. Berdnik, O. M. Dumin, and Y. O. Antonenko, "Asymmetric impedance vibrator for multi-band communication systems," Prog. Electromagn. Res. M, **102**, 81-89 (2021). http://dx.doi.org/10.2528/PIERM21031207
[27] R. Xu, and Z. Shen, "Dual-band circularly polarized RFID reader antenna with combined dipole and monopoles," IEEE Trans. Antennas Propag., 71, 9593-9600, (2023). https://doi.org/10.1109/TAP.2023.3326945
[28] X. Liu, K. Ning, S. Xue, L. Ge, K. W. Leung, and J.-F. Mao, "Printed filtering dipole antenna with compact size and high selectivity," IEEE Trans. Antennas Propag., **72**, 2355-2367, (2024). https://doi.org/10.1109/TAP.2024.3356176
[29] S. A. Schelkunoff, "Theory of antennas of arbitrary size and shape," Proc. IRE, **29**, 493-521 (1941). https://doi.org/10.1109/JRPROC.1941.231669
[30] C.T. Tai, "On the theory of biconical antennas," Journal Applied Phys., **19**, 1155-1160 (1948). https://doi.org/10.1063/1.1715036
[31] S.A. Schelkunoff, *Antennas Theory and Practice*, (Facsimile Publisher, 1952).
[32] T.T. Wu, and R.W.P. King, "The tapered antenna and its application to the junction problem for thin wires," IEEE Trans. Antennas Propag. **24**, 42-45 (1976). https://doi.org/10.1109/TAP.1976.1141274
[33] S.A. Saoudy, and M. Hamid, "Input admittance of a biconical antenna with wide feed gap," IEEE Trans. Antennas Propag. **38**, 1784-1790 (1990). https://doi.org/10.1109/8.102740
[34] S. S. Sandler, and R. W. P. King, "Compact conical antennas for wide-band coverage," IEEE Trans. Antennas Propag. **42**, 436-439 (1994). https://doi.org/10.1109/8.280735
[35] K.-L. Wong, and S.-L. Chien, "Wide-band cylindrical monopole antenna for mobile phone," IEEE Trans. Antennas Propag. **53**, 2756-2758 (2005). https://doi.org/10.1109/TAP.2005.851784
[36] O. Dumin, P. Fomin, V. Plakhtii, and M. Nesterenko, "Ultrawideband combined monopole-slot radiator of Clavin type," in Proc. XXVth Int. Sem. Direct Inverse Problems of Electromagn. and Acoustic Wave Theory, 32-36, (2020). https://doi.org/10.1109/DIPED49797.2020.9273399
[37] P. Fomin, O. Dumin, V. Plakhtii, and M. Nesterenko, "UWB antenna arrays with the monopole-slot radiator of Clavin type," in Proc. IIIth Ukraine Conf. on Electrical and Computer Engineering, 258-261, (2021). https://doi.org/10.1109/UKRCON53503.2021.9575282
[38] M. V. Nesterenko, A. V. Gomozov, V. A. Katrich, S. L. Berdnik, and V. I. Kijko, "Scattering of electromagnetic waves by impedance biconical vibrators in a free space and in a rectangular waveguide," Prog. Electromagn. Res. C, **119**, 275-285 (2022). http://dx.doi.org/10.2528/PIERC22020304
[39] M.S. Fouad, A.E. Farahat, K.F.A. Hussein, A.A. Shaalan, and M.F. Ahmed, "Super-wideband fractal antenna for future generations of wireless communication," Prog. Electromagn. Res. C, **136**, 137-149 (2023). http://dx.doi.org/10.2528/PIERC23042507
[40] F. F. Dubrovka, S. Piltyay, M. Movchan, and I. Zakharchuk, "Ultrawideband compact lightweight biconical antenna with capability of various polarizations reception for modern UAV applications," IEEE Trans. Antennas Propag., **71**, 2922-2929 (2023). https://doi.org/10.1109/TAP.2023.3247145
[41] J.M. Platt, L.B. Boskovic, and D.S. Filipovic, "Wideband biconical antenna with embedded band-notch resonator," IEEE Trans. Antennas Propag., **72**, 2921-2925 (2024). https://doi.org/10.1109/TAP.2024.3349785
[42] I. D. Chiele, M. Donelli, J. Iannacci, and K. Guha, "On chip modulated scattering tag operating at millimetric frequency band," Prog. Electromagn. Res. M, **124**, 71-77 (2024). http://dx.doi.org/10.2528/PIERM23102707
[43] M. V. Nesterenko, V. A. Katrich, and S. V. Pshenichnaya, "Multyband asymmetric biconical dipole antenna with distributed surface impedance and arbitrary excitation," East European J. Physics, **2**, 450-455 (2024). https://doi.org/10.26565/2312-4334-2024-2-59
[44] R.W.P. King, and G.S. Smith, *Antennas in Matter*, (Cambridge, USA: MIT Press, 1981).
[45] R.W.P. King, and L.D. Scott, "The cylindrical antenna as a probe for studying the electrical properties of media," IEEE Trans. Antennas and Propagat., **19**, 406-416 (1971). https://doi.org/10.1109/TAP.1971.1139930
[46] D. Lamensdorf, "An experimental investigation of dielectric-coated antennas," IEEE Trans. Antennas and Propagat. **15**, 767-771 (1967).
[47] *Tables of Physical Values. Handbook*, Editor I. K. Kikoin. (Moskow: Atomizdat, 1976). (in Russian)
[48] K. Yoshitomi, "Radiation frm a slot in an impedance surface," IEEE Trans. Antennas Propag. **49**, 1370-1376 (2001). https://doi.org/10.1109/8.954925

ВИПРОМІНЮВАННЯ ЕЛЕКТРОМАГНІТНИХ ХВИЛЬ РЕГУЛЯРНИМИ ТА БІКОНІЧНИМИ ДИПОЛЯМИ ЗІ ЗМІННИМ РОЗПОДІЛЕНИМ ПОВЕРХНЕВИМ ІМПЕДАНСОМ І ДОВІЛЬНИМ ЗБУДЖЕННЯМ

Михайло В. Нестеренко, Віктор А. Катрич, Юрій В. Аркуша, Володимир В. Катрич
Харківський національний університет імені В.Н. Каразіна, майдан Свободи, 4, Харків, Україна, 61022

Отримано наближений аналітичний розв'язок задачі про випромінювання електромагнітних хвиль регулярними та біконічними диполями з постійним та змінним комплексним розподіленим поверхневим імпедансом і довільним збудженням. Правильність рішення підтверджується задовільним узгодженням експериментальних і чисельних результатів із відомих літературних джерел. Наведено чисельні результати для вхідних характеристик і полів випромінювання диполів у випадках їх симетричного та асиметричного збудження точковим джерелом.

Ключові слова: *регулярний диполь; біконічний диполь; змінний розподілений поверхневий імпеданс; довільне збудження; розподіл струму; вхідні характеристики; поля випромінювання*